

Color-Tunable Triple-State “Smart” Window

Gilles H. Timmermans, Jiajun Wu, Albert P.H.J. Schenning, Jianbin Lin,*
and Michael G. Debije*

Materials that rapidly change their optical properties in response to external stimuli are crucial for displays and “smart” window applications. Herein, a fluorescent red dye modified with liquid crystal (LC) side chains is described to be interactive with a LC host, resulting in a color-tunable triple-state smart window. The dye solubilizes in the LC matrix with increasing temperature, resulting in a red-colored, absorbing state, recovering transparency again by reaggregation of the dye within minutes upon cooling. This dye is used to fabricate a device that can be electrically switched from a red-colored, absorbing state to an intermediate scattering state and at greater electrical fields, a transparent state. Using a second dichroic fluorescent dye, heating the device transitions the window’s color from yellow/green to red. The multiresponsive optical changes could find applications in many fields, including displays, smart windows, electricity generation, and signage.

Switchable properties that are of particular interest are changes in color, transparency, scattering, and/or reflectivity.^[19,20] Potential stimuli of interest as triggers include electrical,^[20–22] thermal,^[23–25] and optical,^[26–28] although there are many other options.^[17,29,30]

A potential deployment that has not been exploited for such “smart” systems is signage. The printed signage market has a multimillion dollar turnover^[31] and is still growing, expected to have a compound annual growth rate of 0.52% for the period 2020–2025.^[32] A highly visible, fluorescence-based sign that may be electrically switched and thermally erased and rewritten with new messages could be quite attractive.

In this work, we propose a device that can alter both its color and transparency in response to both heat and electrical potential, making for a very flexible design. In earlier work, we demonstrated a thermally reversible perylene-core dye in the liquid crystal (LC) blend E7.^[33] While this dye produced reversible color variation upon heating, returning to the transparent state took quite a long time (>45 min), which makes it less viable for use in devices where rapid reversibility is desired. We conjectured that the addition of cyano-biphenyl groups^[34] at the end of the alkyl tails of a perylene core to better match the chemical nature of the host LC E7^[35] would allow both enhanced interaction between the dye and the host LC but also promote more rapid association of the dyes upon cooling. Indeed, we show that cyano-biphenyl groups result in faster dye reaction speeds, while maintaining excellent alignment, and provide an improved electrical response. The new dye combined with a second dichroic dye and a chiral dopant is used to fabricate a color-tunable triple-state “smart” window that is electrically switchable between a dark, “absorbing” state and a transparent state, with an intermediate scattering state and with a thermal override to a bright red color.


1. Introduction

Materials that can alter their optical properties in reaction to external stimuli have received considerable attention as they can be used for a variety of applications, including displays,^[1–4] “smart” windows,^[5–7] and luminescent solar concentrators (LSCs).^[8–11] More recent applications under consideration include greenhouses,^[12–14] camouflage,^[15,16] and sensors.^[17,18]

In “smart” windows, the switchable devices have advantages over standard static systems, allowing different appearances, which may change in time. A fast response is generally desired for windows used in buildings, although the rate of response really depends on the application, where changes in months, days, hours, minutes, seconds, or even milliseconds are all demanded.

Dr. G. H. Timmermans, Prof. A. P. H. J. Schenning, Dr. M. G. Debije
Stimuli-responsive Functional Materials and Devices, Chemical
Engineering & Chemistry
Eindhoven University of Technology
Eindhoven 5600 MB, The Netherlands
E-mail: M.G.Debije@tue.nl

Dr. J. Wu, Dr. J. Lin
Department of Chemistry, College of Chemistry and Chemical Engineering
Xiamen University
Xiamen 361005, China
E-mail: jb.lin@xmu.edu.cn

 The ORCID identification number(s) for the author(s) of this article can be found under <https://doi.org/10.1002/adpr.202100134>.

© 2021 The Authors. Advanced Photonics Research published by Wiley-VCH GmbH. This is an open access article under the terms of the Creative Commons Attribution License, which permits use, distribution and reproduction in any medium, provided the original work is properly cited.

DOI: 10.1002/adpr.202100134

2. Results and Discussion

2.1. CB–Perylene Dye

The synthesis of the novel cyano-biphenyl dye, which we will refer to as CB–perylene (**3**), was done in three steps, as shown in **Figure 1**. The key compound **1** was synthesized via Suzuki coupling between the in situ-formed bis-boron derivative with both 4'-bromo-4-cyano-biphenyl^[36] and 4-bromoaniline sequentially in the same pot. **1** was purified by silica gel column

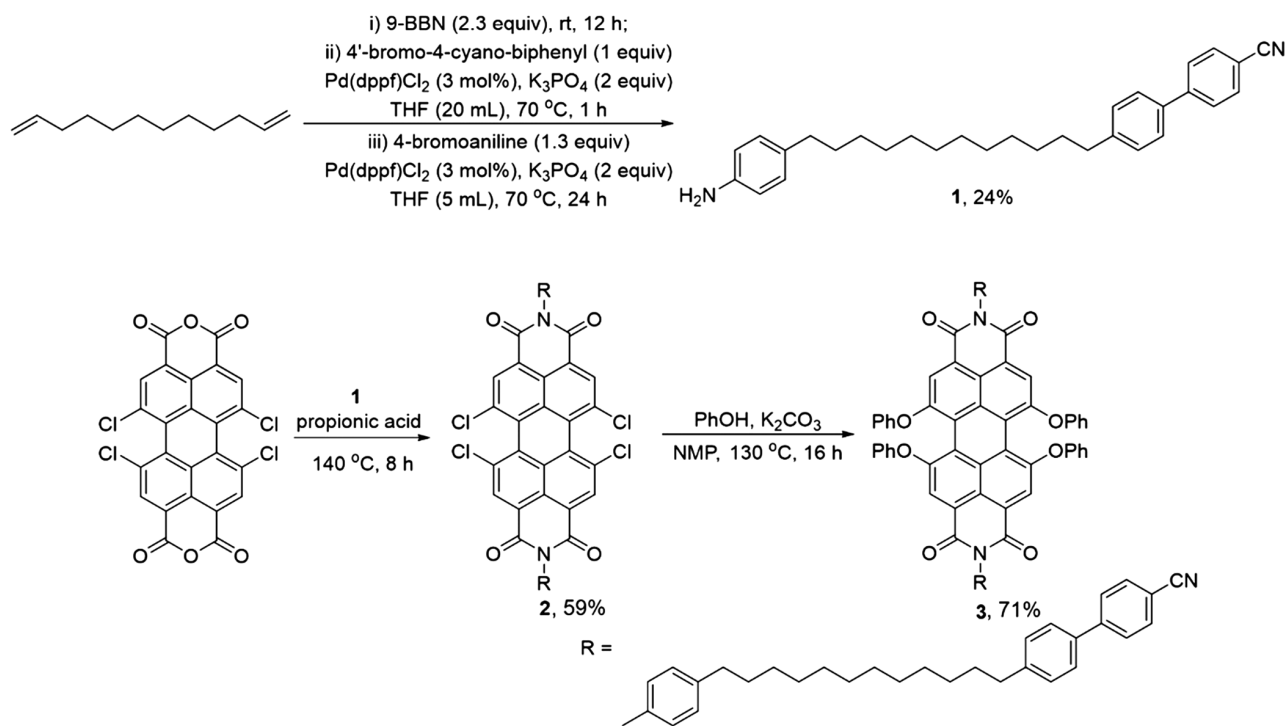


Figure 1. Synthetic route to produce **3**, the CB-perylene.

chromatography using DCM/hexane as the eluent. Following a modified literature protocol,^[37] compound **2** and **3** were obtained in good yields. The detailed procedures are shown as Supporting Information. The target compound CB-perylene was characterized in detail with ^1H and ^{13}C nuclear magnetic resonance (NMR) spectroscopy and high-resolution mass spectrometry (HRMS) (see Figure S3, Supporting Information).

Similar to its predecessor C12-PBI (see Figure 2),^[33] most of the dye aggregates at 0.25 wt% in the nematic host LC E7 at room temperature (see Figure S4, Supporting Information) result in a relatively colorless cell. Upon increasing the temperature to $>55^\circ\text{C}$, the dye mostly dissolves, aligning parallel to the planar LC host. The order parameter (S) of CB-perylene in E7 was measured in the dissolved state, using polarized absorption, and calculated using

$$S = \frac{A_{\text{par}} - A_{\text{per}}}{A_{\text{par}} + 2A_{\text{per}}} \quad (1)$$

where A_{par} and A_{per} are the peak absorbances of the sample, when incident light was polarized parallel and perpendicular to the alignment direction of the host LCs, respectively. We determine a high degree of alignment ($S=0.6$, see Figure S5, Supporting Information), indicating a good interaction between the dye and the E7 host; this value is greater than that found for the coumarin derivative dye labeled **6** in Figure 2, which has been one of the highest reported in E7,^[38,39] and approximately the degree of alignment of the E7 host itself.^[40]

While at room temperature the system is mostly transparent, application of $7 V_{\text{RMS}}$ rotates the E7 host to the homeotropic alignment, realigning the minor amount of nonaggregated

dye, further reducing absorption as the dye is dichroic, and so it absorbs little light when orientated with its molecular long axis directed toward the viewer (see Figure 3). Increasing the temperature allows dye to deaggregate and promote light absorption. As more dye dissolves, more dye can realign when an electrical potential is applied across the cell, reaching a maximum difference between the “on” and “off” states of the window at 55°C (see Figure 4). At 65°C , the E7 host becomes isotropic and no longer responds to the applied electric field.

The recovery of the system to colorless upon cooling from its colored state was measured by first heating the sample to 80°C and measuring the absorption spectra every 5 min as the sample cooled at ambient conditions. The results for CB-perylene show that within 5 min the absorption returns to 88% of its initial value and completely recovers to its initial state at ≈ 25 min (see Figure S6, Supporting Information). In contrast, C12-PBI, which does not boast of the cyano-biphenyl groups, takes much longer to recrystallize: the 88% recovery takes 45 min and still does not reach its minimum value even after 90 min. This rapid recrystallization in CB-perylene is promising for future applications, where quick switching is desired, such as rewriteable message boards (preliminary efforts are shown in Figure S7, Supporting Information).

2.2. Color-Tunable Triple-State “Smart” Window

A method to create a scattering state in a switchable LC system without polymerization is using a “supertwist” system.^[3,10,41,42] In a supertwist system, a small amount of chiral dopant is added to a nematic LC to create several rotations of the LC through the

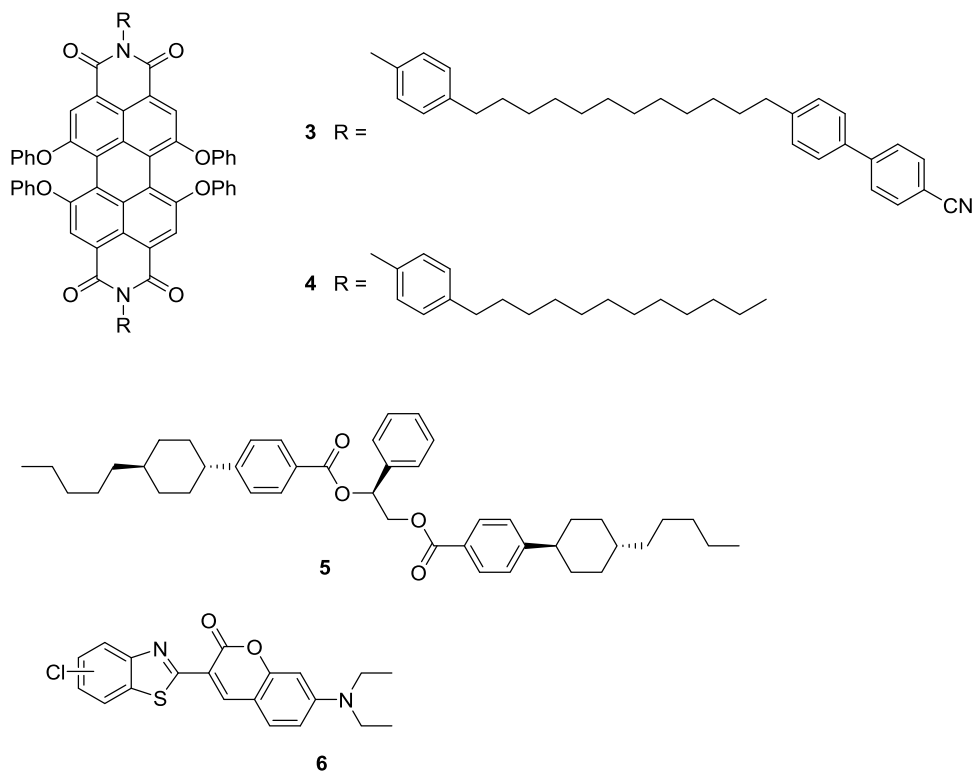


Figure 2. Molecular structure of: 3) dye CB-perylene, 4) dye C12-PBI,^[33] 5) chiral dopant S1011, and 6) the coumarin derivative.

depth of the cell. When applying intermediate voltages, the supertwist hinders the formation of a homeotropic state, resulting in a focal conic (scattering) state; at still higher

voltages, the homeotropic state is generated. Supertwist “smart” windows that use dichroic dyes have increased absorption as a result of multiple alignments throughout the thickness of the samples.^[10]

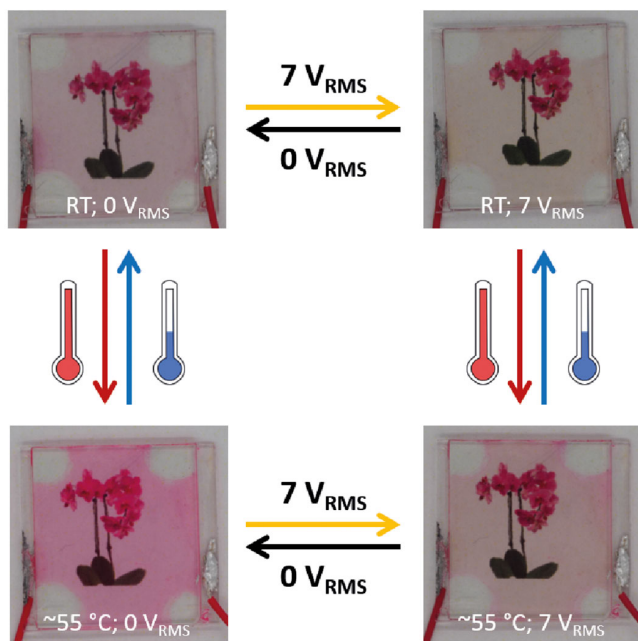


Figure 3. Photographs of a cell containing 0.25 wt% CB-perylene in E7 under various conditions: (top left) RT, 0 V_{RMS} ; (top right) RT, 7 V_{RMS} ; (bottom left) ≈ 55 °C, 0 V_{RMS} ; (bottom right) ≈ 55 °C, 7 V_{RMS} .

To fabricate the “smart” window, we used 0.25 wt% of CB-perylene 3, 0.25 wt% of a fluorescent coumarin derivative 6, and 1 wt% of S1011 chiral dopant 5 (see Figure 2) dissolved in the nematic LC host. When heating the “smart” window, more CB-perylene dye dissolves and the window becomes increasingly red colored (Figure 5a). The dissolution of the red dye clusters was monitored using UV-vis spectroscopy (see Figure 5b). Initially, only the 450 nm absorption peak from the coumarin derivative is visible with some scattering at longer wavelengths caused by the CB-perylene agglomerates. Increasing the temperature results in the dissolving of the CB-perylene clusters and the appearance of the perylene absorption peak with corresponding reduction in scattering, with scattering reaching a minimum at around 60 °C, the isotropic temperature of the mixture (see Figure S8, Supporting Information for the differential scanning calorimetry (DSC)). Application of a voltage (Figure 5c,d shown at RT) below the temperature of the isotropic transition increases the scattering, with a maximum appearing at around 9 V_{RMS} as a focal conic LC state is achieved. Further increasing the potential decreases both the absorption and scattering of the cell as a homeotropic LC state with both the two dichroic dyes aligned perpendicular to the cell surface (see Figure S9, Supporting Information). All electrically driven state transitions, including reverting to the rest state upon turning off the applied voltage, occur in ≈ 1 s (see Video 1, Supporting Information).

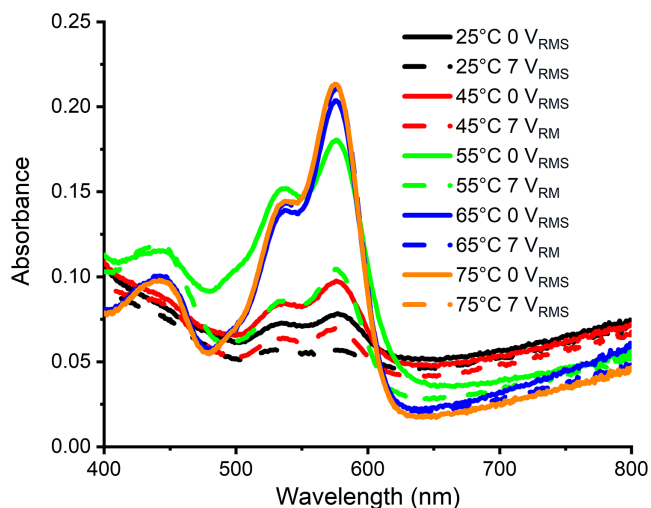


Figure 4. Absorbance spectra of 0.25 wt% CB-perylene in E7 at various temperatures at (solid lines) 0 V_{RMS} and (dashed lines) 7 V_{RMS} .

Not only can the “smart” window be switched independently with temperature or applied voltage, but the two stimuli can also be applied simultaneously (see **Figure 6a**). Below $\approx 60^\circ\text{C}$, the system is responsive to both temperature and electrical fields, after which the LC becomes isotropic and further application of a voltage has no effect. The effect of intermediate temperatures and voltage on the absorption of CB-perylene at 575 nm (corrected for scattering) is shown in **Figure 6b**. The original data are shown in **Figures S10**, Supporting Information.

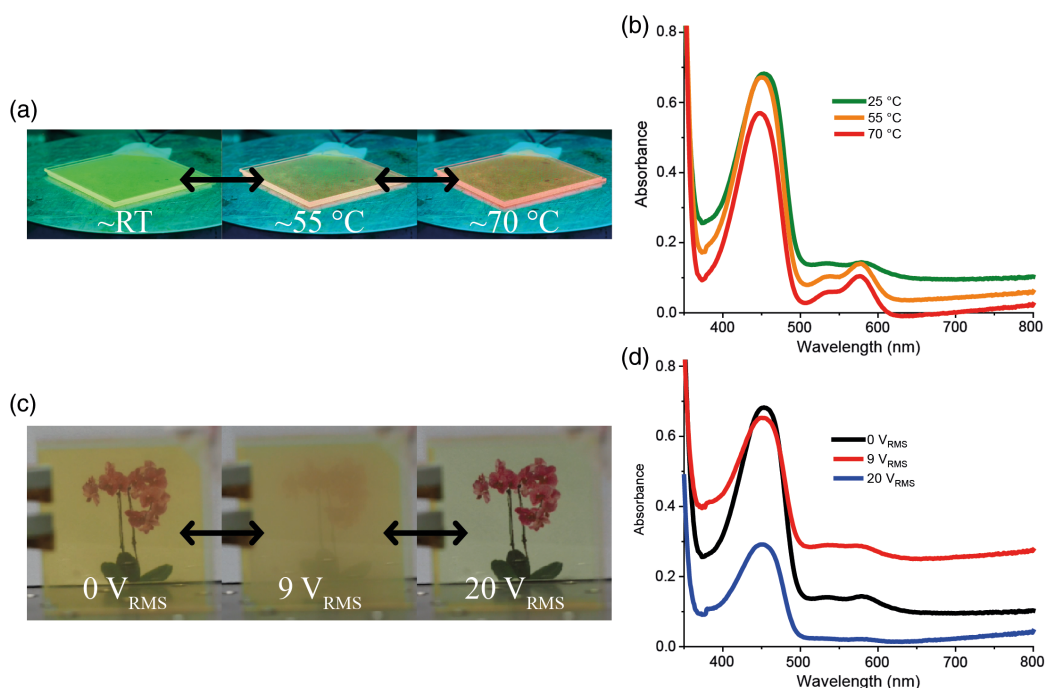


Figure 5. a) Photographs of the dual-dye “smart” window at (from left to right): RT, $\approx 55^\circ\text{C}$, and 70°C . b) Absorption spectra of the “smart” window at the different temperatures and 0 V_{RMS} . c) Photographs of the “smart” window at RT and different applied voltages, from left to right: 0 V_{RMS} , 9 V_{RMS} , and 20 V_{RMS} . d) Absorption spectra of the “smart” window at various applied voltages at RT.

Figure 7 schematically shows the “smart” window in its various states as it responds to changes in both temperature and applied electrical fields. At low temperatures, most of the red CB-perylene dye is aggregated in a nonfluorescent form and the device is colored yellow from the coumarin derivative. Application of an intermediate voltage forms a yellow, scattering texture and at higher voltages a transparent, slightly yellow, state. Increasing the temperature results in a red color as the CB-perylene is dissolved to its fluorescent form and receives energy from the coumarin. At temperatures below the isotropic point of the LC ($< 65^\circ\text{C}$), a red scattering texture and transparent, slightly red colored state is formed upon application of intermediate and high voltages, respectively. When heated above the isotropic temperature, the device can no longer respond to changes in voltage.

The window could be repeatedly switched electrically with no loss in performance after 20 cycles. While no significant changes in the bulk absorbance were obvious after ten heating cycles to 80°C , there was some additional clustering of the CB-perylene visible, suggesting that cycling has to be improved with some modification of the structure, although it is likely that the extreme temperatures used may have played a role (see **Figure S11**, Supporting Information).

To investigate the performance of the “smart” window for electricity generation in LSC-like applications,^[8,43] the edge emissions were measured as a function of temperature and applied voltage when exposed to an AM 1.5 solar spectrum (**Figure S12**, Supporting Information). At the application of 20 V_{RMS} there is a decrease in emission at every wavelength as the sample becomes homeotropic. The emissions of the coumarin derivative (450–580 nm) noticeably decrease with increasing temperature, whereas the emissions of

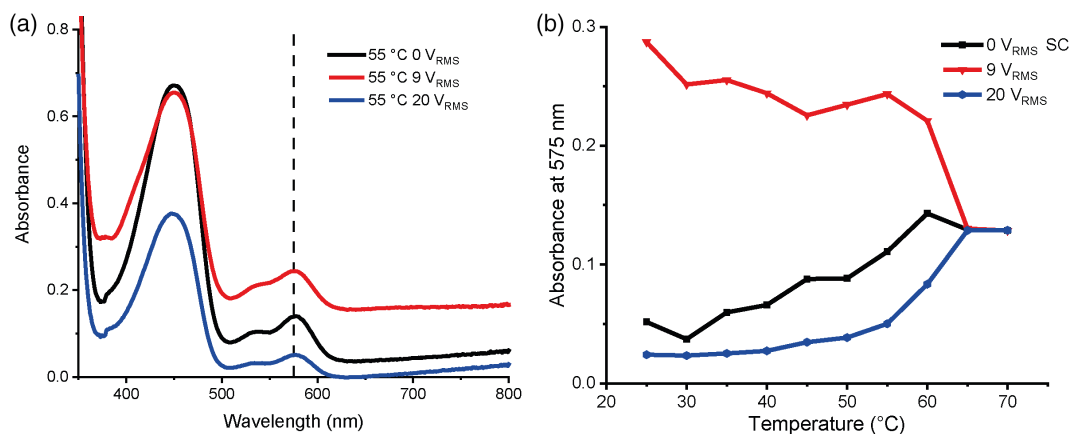


Figure 6. a) Absorption spectra of the “smart” window at 55 °C and 0 V_{RMS} and 9 V_{RMS} and 20 V_{RMS} (with vertical dotted line indicating 575 nm). b) Peak absorbance at 575 nm of the supertwist sample at various temperatures and voltages. The 0 V_{RMS} scattering (SC) is corrected for the scattering (see Figure S8, Supporting Information). Lines are added between points as an aid for the eye.

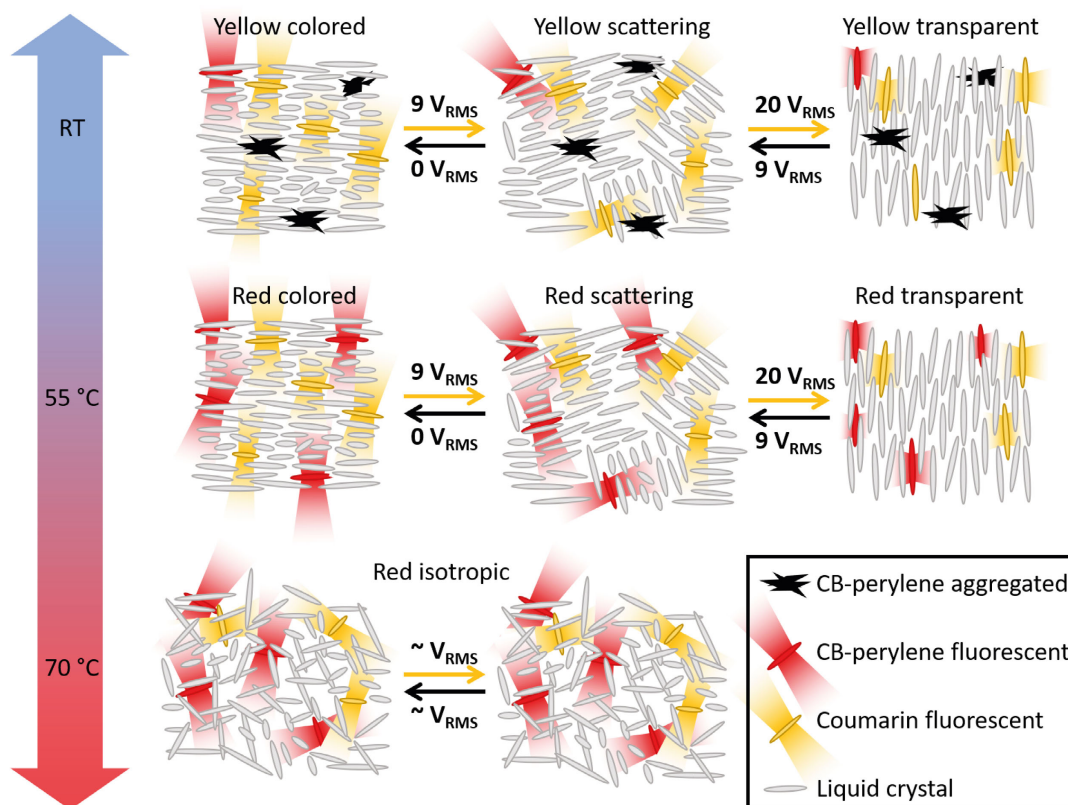


Figure 7. Schematic representation of the different states of the dual-temperature/electrical-responsive “smart” window architecture. From left to right along the top row: conditions under ambient temperature, with the visually yellow state with most CB–perylene aggregated. Upon application of intermediate potential, the LCs take a focal conic, scattering texture. Further potential increase forms the transparent, homeotropic LC alignment. Heating the sample to a higher temperature below the isotropic phase transition leads to (middle row, left to right) a red absorbing state with the CB–perylene accepting this energy transfer from the coumarin. Upon application of intermediate and higher voltages, the focal conic and homeotropic states are attained. Finally, (bottom row) heating the sample to above the isotropic phase transition leads to a random alignment and a red color that is not affected by the application of an electric field.

CB–perylene (580–750 nm) increase. This decrease in coumarin emissions is partially supported by Förster resonance energy transfer (FRET) as CB–perylene is released (see Figure S13 and S14, Supporting Information for details).

3. Conclusion

A fluorescent dye was synthesized to have interaction with its host LC by attaching cyano-biphenyl groups at the end of the alkyl tails on a perylene core. The dye aligns well in the nematic LC host E7, responding to an electrical field and rapidly aggregating at lower temperatures and dissolving at higher temperatures.

Using this dye in combination with a second fluorescent dichroic dye in a supertwist LC system, a color-tunable triple-state “smart” window was fabricated. The “smart” window can change its optical properties both through temperature but also through application of an electrical field. A dramatic color change from green/yellow to brilliant red with a corresponding increase in red edge emission via enhanced fluorescence transfer was achieved by heating the device. A scattering state is generated due to the application of an intermediate voltage; it is possible to override the bright yellow/green or red colors by application of a higher field to generate a transparent system. This system has potential for application as “smart” windows and possibly as visually stunning, rewritable signage.

4. Experimental Section

CB–perylene (4',4'''-(((1,3,8,10-tetraoxo-5,6,12,13-tetraphenoxy-1,3,8,10-tetrahydroanthra[2,1,9-def:6,5,10-d'e'f']diisoquinoline-2,9-diy))bis(4,1-phenylene))bis(dodecane-12,1-diy))bis([1,1'-biphenyl]-4-carbonitrile) **3** was synthesized as described. C12–PBI (2,9-bis(4-dodecylphenyl)-5,6,12,13-tetraphenoxyanthra[2,1,9-def:6,5,10-d'e'f']diisoquinoline-1,3,8,10(2H,9H)-tetraone) **4** was synthesized as described previously.^[33] 0.25 wt% of the dyes were blended in the LC mixture E7 (Merck). For the supertwist experiments, a mixture was made of 0.25 wt% dye **3**, 0.25 wt% of the coumarin derivative (RiskReactor) **6**, and 1 wt% chiral dopant S1011 (Merck) **5** in E7.

Indium tin oxide (ITO)-coated glass plates of 3 × 3 cm² were cleaned and a layer of planar polyimide (OPTMER AL 1051, JSR Corporation, Tokyo, Japan) was spin coated (Karl Suss RC8, 40 s at 5000 rpm) onto the cleaned glass plates, which were then baked for 1.5 h at 180 °C and rubbed over a velvet cloth to induce planar alignment. The cells were fabricated by gluing two rubbed plates together with glue containing 20 μm glass spacer beads in an antiparallel fashion with a small offset at the edges. In addition, custom-made ITO-coated cells (5 × 5 cm² switching area, 20 μm spacing) from LC–Tec Displays AB were also purchased. The cells were filled with the LC mixtures in the isotropic state and allowed to cool and rest for a day before use. The 3 × 3 cm² cells were used for the absorption measurements and the 5 × 5 cm² cells for the edge-emission measurements.

UV–vis absorbance spectra were measured on a PerkinElmer Lambda 750 with a 150 mm integrating sphere. Edge emissions were measured using a Labsphere SLMS 1050 integrating sphere connected to an International Light RPS900 diode array detector. Illumination was provided by a 300 W Lot–Oriol solar simulator equipped with filters to emulate the AM1.5 solar spectrum. Sine-wave voltage modulation at 1000 Hz was applied to the cells using a laboratory function generator (Agilent 33220A) coupled to a 20× voltage amplifier (FLC Electronics F20A) in the range of 0–26 V_{RMS}. The fluorescence lifetime and photoluminescence spectra were obtained with an Edinburgh Instruments LifeSpec-ps spectrophotometer with a Peltier-cooled Hamamatsu microchannel plate photomultiplier for detection and coupled to a 400 nm pulsed laser (PicoQuant LDH–C 400, 2.5 MHz; PicoQuant PDL 800–B driver): for

the excitation of the analyte with power kept below 1 mW using a diaphragm. The fluence of a single pulse was 10^{−8} J cm^{−2}.

Supporting Information

Supporting Information is available from the Wiley Online Library or from the author.

Acknowledgements

The authors would like to acknowledge the support of the TKI PPS Smart Materials for Greenhouses Program. The authors are grateful for financial support from the Natural Science Foundation of China (nos. 21772165 and 22071208).

Conflict of Interest

The authors declare no conflict of interest.

Data Availability Statement

Research data are not shared.

Keywords

dye aggregation, liquid crystals, perylene bisimide, responsive, “smart” windows

Received: May 17, 2021
Published online: August 5, 2021

- [1] J. R. Talukder, H.-Y. Lin, S.-T. Wu, *Opt. Express* **2019**, *27*, 18169.
- [2] P. W. Benzie, S. J. Elston, in *Handbook of Visual Display Technology* (Eds: J. Chen, W. Cranton, M. Fihn), Springer Berlin Heidelberg, Berlin, Heidelberg **2012**, pp. 1365–1385.
- [3] S. C. Guy, *Displays* **1993**, *14*, 32.
- [4] I. Papakonstantinou, M. Portnoi, M. G. Debije, *Adv. Energy Mater.* **2021**, *11*, 2002883.
- [5] Y. Zhan, H. Lu, M. Jin, G. Zhou, *Liq. Cryst.* **2019**, *00*, 1.
- [6] J. R. Talukder, Y.-H. Lee, S.-T. Wu, *Opt. Express* **2019**, *27*, 4480.
- [7] Y. Zhang, C. Y. Tso, J. S. Iñigo, S. Liu, H. Miyazaki, C. Y. Chao, K. M. Yu, *Appl. Energy* **2019**, *254*, 113690.
- [8] M. G. Debije, *Adv. Funct. Mater.* **2010**, *20*, 1498.
- [9] G. Griffini, *Front. Mater.* **2019**, *6*, 1.
- [10] J. A. H. P. Sol, G. H. Timmermans, A. J. van Breugel, A. P. H. J. Schenning, M. G. Debije, *Adv. Energy Mater.* **2018**, *8*, 1702922.
- [11] B. McKenna, R. C. Evans, *Adv. Mater.* **2017**, *29*, 1606491.
- [12] C. Corrado, S. W. Leow, M. Osborn, I. Carbone, K. Hellier, M. Short, G. Alers, S. A. Carter, *J. Renewable Sustainable Energy* **2016**, *8*, 043502.
- [13] G. H. Timmermans, S. Hemming, E. Baeza, E. A. J. van Thoor, A. P. H. J. Schenning, M. G. Debije, *Adv. Opt. Mater.* **2020**, *8*, 2000738.
- [14] E. Baeza, S. Hemming, C. Stanghellini, *Biosyst. Eng.* **2020**, *193*, 157.
- [15] E. Karshalev, R. Kumar, I. Jeerapan, R. Castillo, I. Campos, J. Wang, *Chem. Mater.* **2018**, *30*, 1593.
- [16] M. Moirangthem, A. P. H. J. Schenning, *ACS Appl. Mater. Interfaces* **2018**, *10*, 4168.

- [17] D. J. Mulder, A. P. H. J. Schenning, C. W. M. Bastiaansen, *J. Mater. Chem. C* **2014**, 2, 6695.
- [18] M. Moirangthem, R. Arts, M. Merckx, A. P. H. J. Schenning, *Adv. Funct. Mater.* **2016**, 26, 1154.
- [19] T. J. White, M. E. McConney, T. J. Bunning, *J. Mater. Chem.* **2010**, 20, 9832.
- [20] H. Khandelwal, R. C. G. M. Loonen, J. L. M. Hensen, M. G. Debije, A. P. H. J. Schenning, *Sci. Rep.* **2015**, 5, 11773.
- [21] H. Khandelwal, M. G. Debije, T. J. White, A. P. H. J. Schenning, *J. Mater. Chem. A* **2016**, 4, 6064.
- [22] C. Binet, M. Mitov, M. Mauzac, *J. Appl. Phys.* **2001**, 90, 1730.
- [23] S.-W. Oh, S.-H. Kim, T.-H. Yoon, *Adv. Sustain. Syst.* **2018**, 2, 1800066.
- [24] A. J. J. Kragt, D. J. Broer, A. P. H. J. Schenning, *Adv. Funct. Mater.* **2017**, 28, 1704756.
- [25] E. P. A. van Heeswijk, T. Meeran, J. de Heer, N. Grossiord, A. P. H. J. Schenning, *ACS Appl. Polym. Mater.* **2019**, 1, 3407.
- [26] G. H. Timmermans, B. W. H. Saes, M. G. Debije, *Appl. Opt.* **2019**, 58, 9823.
- [27] T. J. White, R. L. Bricker, L. V. Natarajan, N. V. Tabiryan, L. Green, Q. Li, T. J. Bunning, *Adv. Funct. Mater.* **2009**, 19, 3484.
- [28] S.-W. Oh, S.-H. Kim, T.-H. Yoon, *Sol. Energy Mater. Sol. Cells* **2018**, 183, 146.
- [29] E. P. A. van Heeswijk, A. J. J. Kragt, N. Grossiord, A. P. H. J. Schenning, *Chem. Commun.* **2019**, 55, 2880.
- [30] X. Wang, M. Li, D. Wang, H. Zhang, R. Duan, D. Zhang, B. Song, B. Dong, *ACS Appl. Mater. Interfaces* **2020**, 12, 15695.
- [31] JCDecaux, <https://www.jcdecaux.com/press-releases/full-year-2019-revenue> (accessed: Dec 2020).
- [32] Mordor Intelligence, <https://www.mordorintelligence.com/industry-reports/printed-signage-market> (accessed: Dec 2020).
- [33] J. A. H. P. Sol, V. Dehm, R. Hecht, F. Würthner, A. P. H. J. Schenning, M. G. Debije, *Angew. Chemie Int. Ed.* **2018**, 57, 1030.
- [34] A. Ghanadzadeh, *J. Mol. Liq.* **2003**, 102, 365.
- [35] A. R. E. Brás, S. Henriques, T. Casimiro, A. Aguiar-Ricardo, J. Sotomayor, J. Caldeira, C. Santos, M. Dionísio, *Liq. Cryst.* **2007**, 34, 591.
- [36] S. Ahn, S. Yamakawa, K. Akagi, *J. Mater. Chem. C* **2015**, 3, 3960.
- [37] F. Würthner, A. Sautter, J. Schilling, *J. Org. Chem.* **2002**, 67, 3037.
- [38] P. P. C. Verbunt, A. Kaiser, K. Hermans, C. W. M. Bastiaansen, D. J. Broer, M. G. Debije, *Adv. Funct. Mater.* **2009**, 19, 2714.
- [39] M. G. Debije, C. Menelaou, L. M. Herz, A. P. H. J. Schenning, *Adv. Opt. Mater.* **2014**, 2, 687.
- [40] B. Bahadur, R. K. Sarna, V. G. Bhide, *Mol. Cryst. Liq. Cryst.* **1982**, 72, 139.
- [41] J.-W. Huh, B.-H. Yu, J. Heo, T.-H. Yoon, *Appl. Opt.* **2015**, 54, 3792.
- [42] K.-H. Kim, H.-J. Jin, K.-H. Park, J.-H. Lee, J. C. Kim, T.-H. Yoon, *Opt. Express* **2010**, 18, 16745.
- [43] M. G. Debije, P. P. C. Verbunt, *Adv. Energy Mater.* **2012**, 2, 12.